CREEP LIFE PREDICTION OF CERAMIC COMPONENTS USING THE FINITE ELEMENT BASED INTEGRATED DESIGN PROGRAM (CARES/*CREEP*)*

OSAMA M. JADAAN
University of Wisconsin-Platteville
Platteville, Wisconsin

Lynn M. Powers**
Case Western Reserve University
Cleveland, Ohio

and

John P. Gyekenyesi
NASA Lewis Research Center
Cleveland, Ohio

Introduction and Theory

The desirable properties of ceramics at high temperatures have generated interest in their use for structural applications such as in advanced turbine systems. Design lives for such systems can exceed 10,000 hours. Such long life requirements necessitate subjecting the components to relatively low stresses. The combination of high temperatures and low stresses typically places failure for monolithic ceramics in the creep regime (ref 1).

The objective of this work is to present a design methodology for predicting the lifetimes of structural components subjected to multiaxial creep loading. This methodology utilizes commercially available finite element packages and takes into account the time varying creep stress distributions (stress relaxation). In this methodology, the creep life of a component is divided into short time steps, during which, the stress and strain distributions are assumed constant. The damage, D, is calculated for each time step based on a modified Monkman-Grant creep rupture criterion (ref 2). For components subjected to predominantly tensile loading, failure is assumed to occur when the normalized accumulated damage at any point in the component is greater than or equal to unity.

Some ceramic components, such as vanes and rotors, are subjected to concurrent tensile and compressive stress fields. For such components, failure generally starts at or near the most highly stressed point and subsequently propagates across the section. The creep rupture life for members subjected to concurrent tensile and compressive loading is divided into two stages. The first is called the stage of latent failure (damage initiation). During this stage, the damage accumulates

1

until it reaches unity at some point within the component, and failure begins. Hence, this portion of life for members subjected to concurrent tensile and compressive loading represents the entire-predicted life for predominantly tensile components. Damage due to compressive stresses is assumed to be negligible, although in this methodology, it can be accounted for very easily if it is determined to be of any significance. Subsequently, the second stage, named the damage propagation takes place. During this stage a damage front defined by the condition D=1 will travel through the body or surface of the component. Component failure occurs at the end of this stage when its total load carrying capacity is expended. In CARES/*Creep* (Ceramics Analysis and Reliability Evaluation of Structures/*Creep*), this means that failure is assumed to occur when D=1 at the periphery of the expanded critical damage zone. The corresponding time will be the creep rupture life for that component. This size of the critical damage zone corresponding to creep rupture failure varies depending on the load conditions and component configuration. One estimation for the duration of the propagation stage is to assume it equal to the time it takes the damage zone to penetrate the initial tensile stressed portion of the structure.

Two examples were chosen to demonstrate the viability of the creep life prediction methodology presented above. The integrated design code CARES/*Creep* (Fig. 7) which utilizes this damage accumulation model was used for this purpose. The first example, silicon nitride NCX-5100 notched tensile specimen, represents the application of this approach to predicting the creep rupture life for components subjected to multiaxial predominantly tensile creep loading. The second example, siliconized silicon carbide KX01 bend specimen, represents the application of this approach to components subjected to uniaxial tensile-compressive creep loading. It was found that the methodology described in this paper yielded good creep rupture life predictions for both examples, given the amount of scatter usually found in the creep rupture life data.

<u>Examples</u>

<u>1) Notched Tensile Specimen:</u>
The creep experiments were conducted on two types of silicon nitride NCX-5100 specimens. First, smooth tensile tests were investigated in order to characterize the creep response of the silicon nitride. Second, experiments on notched tensile bars (Fig. 8) provided a multiaxial stress state, especially near the notch root, where the creep life may be predicted from data obtained from the smooth tensile specimens. Creep data used in this example were obtained from ref 3.

Using CARES/*Creep*, the secondary creep rate parameters, C_7, C_8, and C_{10}, were determined to be $7.858 \times 10^{-26}/Pa^{6.75}$ hour, 6.75, and 127560°K, respectively. Figure 9 shows the experimental secondary creep strain rate vs. the analytical secondary creep strain rate. This figure shows that the data scatters relatively close to the 45° line, indicating that the Norton secondary creep rate model (Fig. 9) was successful in describing the secondary creep behavior of the NCX-5100 material.

Four notched bars were tested (ref 3). The reduced section average stresses were 105, 120, 135, and 150 MPa. The maximum principal stress distribution for the 120 MPa reduced average section stress specimen as a function of time is shown in Fig. 10. A multiaxial stress state exists

Paper 16

in the vicinity of the notch root, while the stress state away from the notch is constant and uniaxial. When the load is initially applied, time=0, the maximum principal stress is located at the root of the notch. As time progresses, the stress relaxes and, the local maximum moves into the interior of the notched bar. This stress relaxation, which occurs due to nonlinear creep deformation, will influence the damage calculations. This is because it was found that the location of the maximum cumulative damage also moves away from the surface as time elapses, indicating that failure could originate at the interior of the specimen.

The Monkman-Grant criterion in association with the damage model was used to predict the creep life for the notched specimens. Since this component is entirely subjected to tensile stress state, failure was assumed to occur when D first reached unity at any point. The Table shown in Fig. 11 gives a summary of the failure predictions for the notched bars as a function of their reduced section stress. The predicted lives using the methodology described in this paper and computed via CARES/*Creep* for these specimens compare well to the experimental failure times. Figure 11 also shows a cumulative damage map for the 120 MPa specimen after 80 hours. The cumulative damage is equal to one and is located near to but not directly the root of the notch.

2) Bend bar
This example is presented to demonstrate the methodology discussed in this paper for predicting the creep life of ceramic components subjected to simultaneous tensile/compressive stresses. Wiederhorn et al. (ref 4) conducted creep testing on the KX01 siliconized silicon carbide material at 1300°C using flexure, tensile and compressive specimens. They found that this material spent most of its life in the secondary creep region. Further, they found that the KX01 material displays significant asymmetric creep behavior, and that in both tension and compression, the creep rate displayed a bilinear power (Norton) law behavior with a transition point at a threshold stress (Fig. 13). In this example, CARES/*Creep* was used to predict the creep lives of four point bend specimens using the tensile and compressive creep and creep rupture properties of the material. These predicted lives were then compared to the experimental ones.

Figure 14 displays the evolution of stress as function of time (stress relaxation) for the bar tested at 250 MPa. The stress distribution in the bend bar converged to its stationary value ten hours after the load was applied. This figure also shows how the neutral axis shifts towards the compressive region as the specimen creeps.

Figure 15 show the evolution of damage in the flexure bar tested at 250 MPa initially, at t=14.5 hours corresponding to the time when the damage first reached unity (latent stage of failure), and at t=80 hours corresponding to the time when the final predicted failure occurred (end of damage propagation stage). In this analysis, it was assumed that failure would occur when the initial portion of the bend bar stressed in tension is damage (half the depth). The table shown in Fig. 16 indicates that excellent agreement between experimental and predicted creep lives exists for the bend bars.

Several advantages are apparent to this creep rupture life methodology. First, this methodology yields a cumulative damage map for the component showing the critical locations where failure

Paper 16

would originate. This capability is very helpful in the redesign of such components. In creep type loading applications, it is not a trivial task to predict the location of failure since the multiaxial stress components redistribute as time elapses. Thus, failure will not necessarily occur at the location where stresses are highest at the beginning of loading or at the time of failure, but can take place elsewhere, as shown by the notched tensile specimen. Second, this design methodology is capable of incorporating the primary creep strain effect into the analysis (influences the stress state) which could predict shorter lives (conservative predictions) compared to when only the secondary creep stain effect is used. Third, any equivalent stress criterion can be used to predict the component's life. As multiaxial creep data emerge in the future and we understand better how ceramics fail under such applications, the CARES/*Creep* code can be modified accordingly. Fourth, any creep rupture criterion (Continuum damage mechanics, Larson-Miller, minimum commitment method, etc.) can be utilized to compute the damage and predict life.

References

1. Wiederhorn, S.; Quinn, G.; and Krause, R.: "Fracture Mechanism Maps: Their Applicability to Silicon Nitride," *Life Prediction Methodologies and Data for Ceramic Materials*, ASTM STP-1201, Brinkman, C. R., and Duffy, S. F., eds., American Society for Testing and Materials, Philadelphia, pp. 36-61, 1993.

2. Powers, L. M.; Jadaan, O. M.; Gyekenyesi, J. P.: "Creep Life of Ceramic Components Using a Finite Element Based Integrated Design Program (CARES/*Creep*)," ASME paper 96-GT-369, 1996.

3. White, C.; Vartabedian, A; Wade, J; and Tracey, D: "Notched Tensile Creep Testing of Ceramics," *Materials Science and Engineering*, A203, 217-221, 1995.

4. Wiederhorn, S. M.; Roberts, D. E.; Chuang, T.-J.; and Chuck, L.: "Damage Enhanced Creep in a Siliconized Silicon Carbide: Phenomenology," *Journal of American Ceramic Society*, Vol. 71, pp. 602-608, 1988.

Objective

To develop an integrated design program for predicting the lifetime of structural ceramic components subjected to multiaxial creep loads. This methodology utilizes commercially available finite element packages and takes into account the time varying creep stress distribution (stress relaxation).

Fig. 1

Constitutive Creep Laws

Total Creep Strain

$$\varepsilon_{cr} = \varepsilon_{Primary} + \varepsilon_{Secondary}$$

Primary Creep Strain Increment — Bailey–Norton Law

$$\Delta\varepsilon_p = C_1\,\sigma^{C_2}\,t^{C_3}\,exp\left[-\frac{C_4}{T}\right]\Delta t$$

Secondary Creep Strain Increment — Norton Law

$$\Delta\varepsilon_s = C_7\,\sigma^{C_8}\,exp\left[-\frac{C_{10}}{T}\right]\Delta t$$

where σ is the stress
       t   is the time
       T   is the absolute temperature
       C_i are experimentally determined constants

Fig. 2

Paper 16

Multiaxial Creep Model

Flow Rule

$$\dot{\varepsilon}_{ij}^{cr} = \lambda \, S_{ij}$$

Proportionality Constant

$$\lambda = \frac{3}{2\sigma_e} \, \frac{d\,\bar{\varepsilon}^{cr}}{dt}$$

Secondary Creep Strain Rate

$$\dot{\varepsilon}_{ij}^{cr} = \frac{3}{2} \, S_{ij} \, C_7 \, \sigma_e^{C_8 - 1} \, \exp\left[-\frac{C_{10}}{T}\right]$$

where S_{ij} is the deviatoric stress

Fig. 3

Effective Stress

$$\sigma_e = \frac{1}{\sqrt{2}} \{(\sigma_1 - \sigma_2)^2 + (\sigma_2 - \sigma_3)^2 + (\sigma_3 - \sigma_1)^2\}^{1/2}$$

Effective Secondary Creep Strain

$$\bar{\varepsilon}^{cr} = C_7 \, \sigma_e^{C_8} \, t \, \exp\left[-\frac{C_{10}}{T}\right]$$

where σ_1, σ_2, and σ_3 are the principal stresses

Fig. 4

6

Creep Rupture

Monkman–Grant

$$t_f = b_1 \, \dot{\varepsilon}_s^{-b_2}$$

Modified Monkman–Grant
        Temperature Stratification

$$\ln t_f = d_1 - d_2 \ln \dot{\varepsilon}_s + \frac{d_3}{T}$$

where b_i and d_i are constants

Fig. 5

Damage Assessment

Damage

$$0 \le D \le 1$$

where   D = 0 for an undamaged component
          D = 1 for a failed component

$$D = \sum_{i=1}^{N} \frac{\Delta t_i}{\exp\left[\, d_1 - d_2 \ln \dot{\varepsilon}_{s_i} + d_3/T_i \,\right]}$$

where Δt_i is the duration of the ith time step
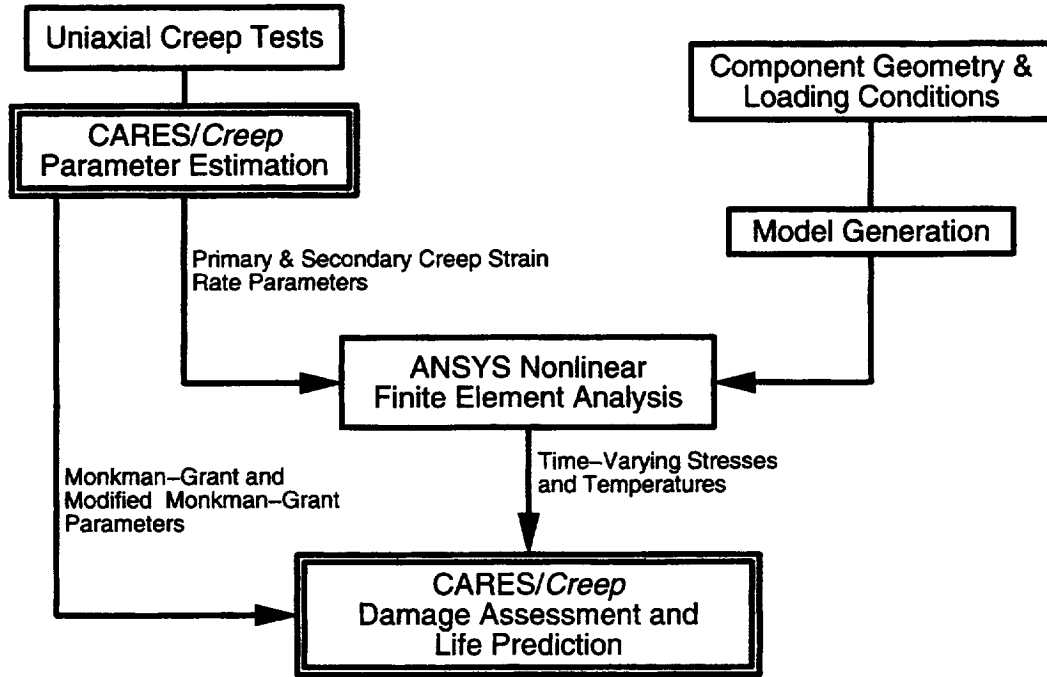   N is the number of time steps

Fig. 6

Integrated Design Program

Uniaxial Creep Tests

CARES/*Creep*
Parameter Estimation

Component Geometry &
Loading Conditions

Model Generation

Primary & Secondary Creep Strain
Rate Parameters

ANSYS Nonlinear
Finite Element Analysis

Monkman–Grant and
Modified Monkman–Grant
Parameters

Time–Varying Stresses
and Temperatures

CARES/*Creep*
Damage Assessment and
Life Prediction

Fig. 7

CARES/*Creep* Multiaxial Tensile Creep Benchmark

Notched Tensile Specimen – Norton Company

Axisymmetric Model
1047 PLANE82 elements

NCX–5100 Silicon Nitride

Axisymmetric Model

Temperature = 1370°C

Constant Applied Load
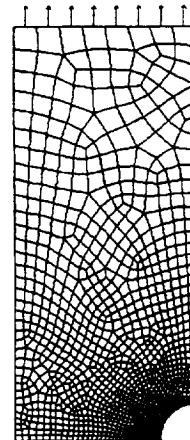
Height = 8.9 cm
Model Height = 0.72 cm
Diameter = 0.32 cm
Notch Radius = 0.032 cm

Fig. 8

8

Parameter Estimation

Silicon Nitride - N CX-5100

37 Tensile Specimen s

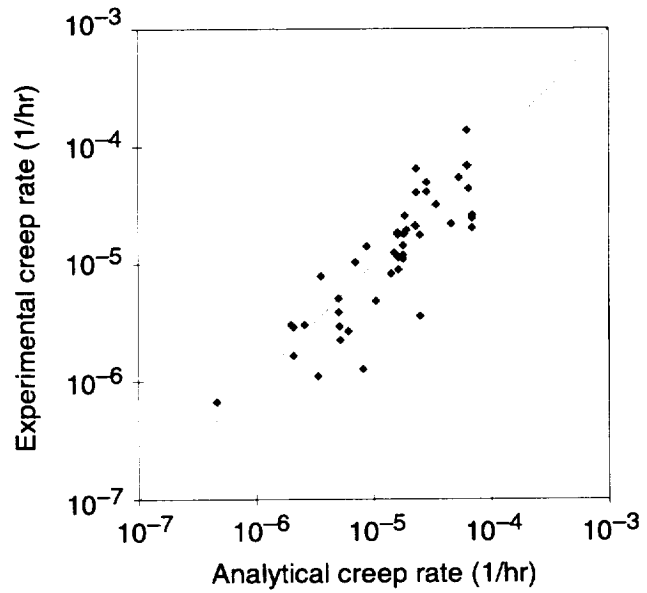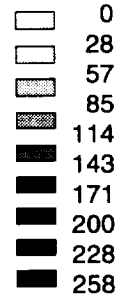Temperatures = 1275-1425 ^{o}C

Applied Load = 120-250 MPa

Fig. 9

Stress Relaxation Near the Notch Root
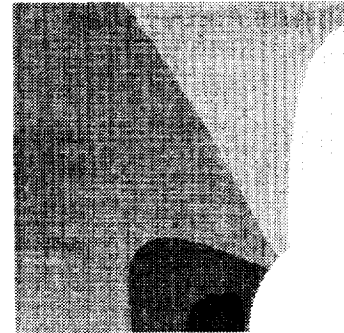
Nominal Reduced Section Stress=120 MPa

MPa
0
28
57
85
114
143
171
200
228
258

Equivalent Stress

Time = 0 hours   10 hours   100 hours

Fig. 10

9

Notched Tensile Specimen

Damage Map

Damage

□	0
▨	0.11
▨	0.22
▨	0.34
▨	0.45
■	0.56
■	0.68
■	0.79
■	0.90
■	1.01

Results

Nominal Reduced Section Stress (MPa)	Experimental Failure Time (hours)	Predicted Lifetime (hours)
105	314	179
120	44	80
135	39	42
150	3.5	17

Secondary Creep
Monkman-Grant Criterion

Fig. 11

CARES/*Creep* Uniaxial Tensile – Compressive Creep Benchmark

Flexural Specimen – NIST

KX01 Siliconized Silicon Carbide

Plane Stress Model
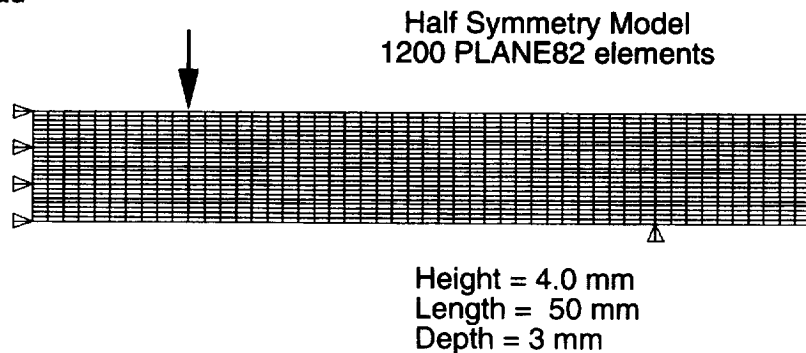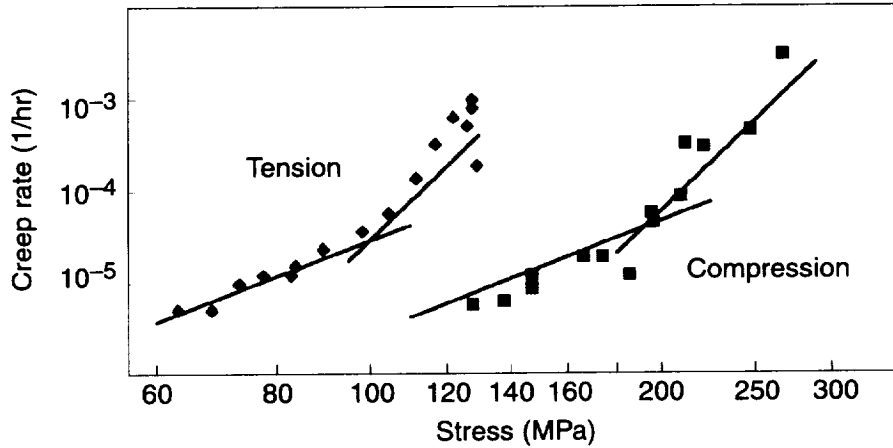
Temperature = 1300°C

Constant Applied Load

Half Symmetry Model
1200 PLANE82 elements

Height = 4.0 mm
Length = 50 mm
Depth = 3 mm

Fig. 12

Parameter Estimation

Siliconized Silicon Carbide - KX01
Uniaxial Tension and Compression Tests at 1300°C

Material displays asymmetric bilinear creep behavior in tension and compression
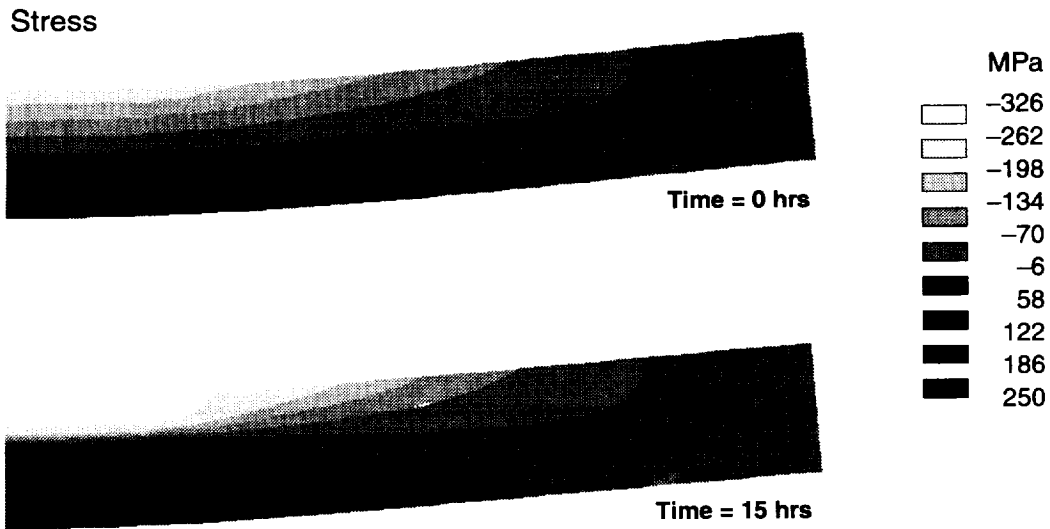
Fig. 13

Stress Relaxation

Maximum Elastic Stress=250 MPa

Fig. 14

Paper 16

Maximum Elastic Stress=250 MPa

MPa
- 0
- .113095
- .226189
- .339284
- .452379
- .565473
- .678568
- .791663
- .904757
- 1.018

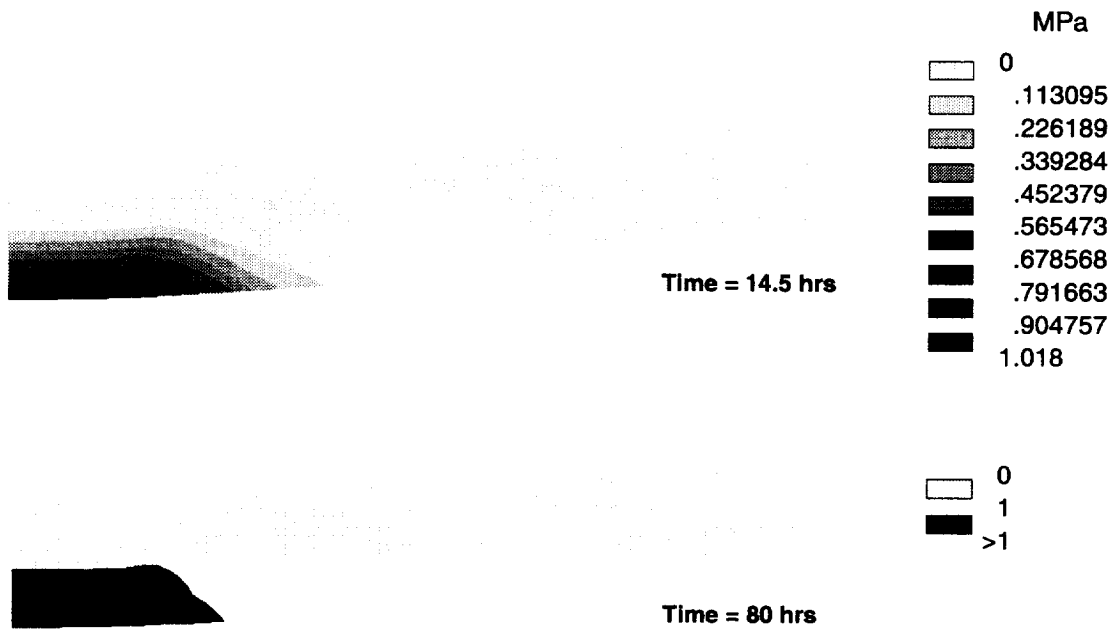**Time = 14.5 hrs**

0
1
>1

Time = 80 hrs

Fig. 15

Flexure Specimen

Results

Initial Maximum Elastic Stress (MPa)	Experimental Failure Time (hours)	Damage Initiation (hours)	Predicted Lifetime (hours)
200	830	200	830
250	55	14.5	80
300	12	1.2	8.6
350	1.3	0.12	1.3

Secondary Creep
Monkman–Grant Criterion

Fig. 16

Summary and Conclusions

A general purpose creep life prediction code, CARES/*Creep*, has been developed. It is integrated with ANSYS finite element software, and can be used to design monolithic ceramic components.

Creep life was predicted based on accumulated damage and the Monkman–Grant and the Modified Monkman–Grant failure criteria.

The creep life was well predicted for components subjected to multiaxial tensile and uniaxial tensile–compressive stress states.

Life prediction for a component with simultaneous tensile–compressive stress states is a two step process involving damage initiation and propagation.

This creep life prediction methodology results in damage maps showing critical regions and, hence, can be used in the components design.

Fig. 17

Focus of Future Research

Creep Response
    Multiaxial Tensile–Compressive Modeling
    Continuum Damage Mechanics

Creep Rupture
    Probabilistic Methods
    Creep–Fatigue Interaction
    Integration with CARES/*Life*

Fig. 18

13